# Hydrogen from urea-water and ammonia-water solutions

Andrew N. Rollinson[†], Gavin L. Rickett[†], Amanda Lea-Langton[†], Valerie Dupont[†]*,

Martyn V. Twigg[‡]

[†]*Energy and Resources Research Institute, University of Leeds, Leeds, LS2 9JT, UK;*

[‡]*Johnson Matthey Orchard Laboratory, Orchard Road, Royston, SG8 5HE, UK*

**Corresponding author: V.Dupont@leeds.ac.uk**

**Abstract:**

The conversion of urea-water into hydrogen was investigated in a downward flow packed-bed reactor using a $Ni-Al_2O_3$ catalyst. This was conducted at atmospheric pressure under molar steam to carbon ratios (S:C) of 4 to 7, and at temperatures between 500 and 700 °C. The urea and water conversions, selectivity to the hydrogen containing products $H_2$, $CH_4$ and $NH_3$, selectivity to the carbon containing products $CO_2$, CO and $CH_4$, and the hydrogen yield, were very close to the calculated equilibrium values at and above S:C of 5 and temperatures at and above 600 °C. $CO_2$ dominated the carbon products, in agreement with equilibrium trends. The selectivity to ammonia decreased abruptly from 20% to below 5% when the temperature increased from 500 to 550 °C, and exhibited a small sensitivity to the steam to carbon ratio. High selectivity to $NH_3$ was accompanied by a low urea conversion to CO, $CO_2$ and $CH_4$, and poor hydrogen yield below 500 °C. Up to 99.3% of

the ammonia generated was easily separated from the syngas by condensation in the excess water. Experiments replacing the Ni-bed with $Al_2O_3$ pellets showed no significant $H_2$ yield, while the main H-product was overwhelmingly $NH_3$. Aqueous Ammonia cracking experiments indicated a reaction further away from equilibrium than the equivalent urea-water experiments, indicative of a hydrogen formation mechanism from urea-water that was more than just a sequence of urea decomposition, HNCO hydrolysis and $NH_3$ cracking. Looking for signs of deactivation, the catalyst was characterised with $N_2$ adsorption, TEM-EDX, and powder XRD. NiO was shown to be present in negligible amounts after the experiments, while crystallite sizes and surface area were not affected significantly, and no coking was observed, evidencing a robust catalyst for this reaction.

# 1. Introduction

The future hydrogen economy requires vectors of renewable hydrogen which can be stored and transported to end-use processes safely and economically. Urea has several advantages over proposed hydrogen carrier compounds to date. It is non-flammable, non-toxic, stable, odourless, and is in crystalline solid form at room temperature, enabling easy storage and transport -with only dry containment being required. This is an immediate advantage over other hydrogen carriers such as ammonia ($NH_3$), which is a toxic gas, or methyl-cyclohexane, which produces benzene as a by-product during its decomposition to hydrogen. The potential of urea as a safe and sustainable hydrogen carrier has been explored in [1], whose findings are summarised below.

As a $H_2$ carrier, urea has a gravimetric hydrogen content of 6.71 wt%, fulfilling present DOE targets for hydrogen storage in transport applications [2]. With the additional molecule of $H_2$ available when the stoichiometric amount of water is included, the value becomes 7.95 wt% of stoichiometric urea-water solution, or 10.07 wt% on the basis of the urea content alone. If a molar water to carbon ratio of 3 was used, the gravimetric content would still be 5.3 wt% of the combined urea and water.

There are many routes that may yield renewable urea. Most attractively, it is secreted in the urine of mammals and all other animals, e.g. fish, amphibians, zooplankton and bacteria [3-7], except birds and saurian reptiles. It is approximately in 2 wt% concentration in human urine, representing a molar ratio of water to carbon of 159. Plants also synthesise urea, where it is believed to be a nitrogen store [8]. Urea is biodegradable and long-term human exposure studies indicated it is non-allergenic, having no side effects [9]. Its biodegradation is rapid upon contact with soil and water. Using urine diversion toilets [10,11], the collected undiluted-urine could be stabilised with a mild acid to prevent its decomposition to ammonia [10], and the urea water solution concentrated by evaporation

3

using lower grade waste heat. This would aim to reach conditions where the urea would precipitate, be collected, stored or transported in dry crystal form. Alternatively, it would be allowed to reach the optimum water to carbon ratio for maximum hydrogen yield. The storage and transport of urea requires very dry, ambient temperature conditions. At present, urea is a widely available commodity with commercial production plants operating the well-established reaction of ammonia ($NH_3$) with carbon dioxide ($CO_2$) via ammonium carbamate at elevated temperature and pressure, a process which has been suggested as a means of recycling the greenhouse gas $CO_2$ [12].

$$CO_2 + 2NH_3 \rightarrow NH_2COONH_4 \rightarrow (NH_2)_2CO + H_2O \quad \Delta H°_{298} = -102 \text{ kJ mol}^{-1}$$
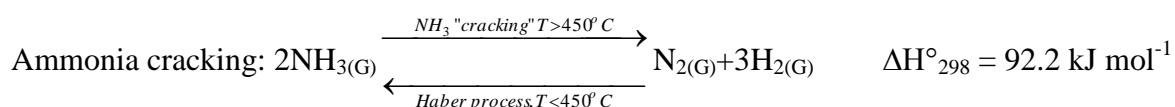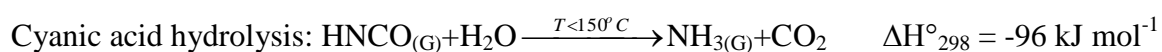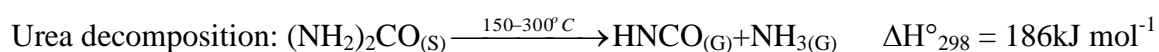
The global demand for urea as slow release fertiliser is growing, with an expected rise of 30.2 Mt from 150Mt in 2008 to 180Mt in 2012 [13]. It is also increasingly used to control nitrogen oxides emissions in the atmosphere via selective catalytic reduction (SCR) [14-16]. The investigation of the SCR process has spurred most of the research into the mechanism of urea decomposition and hydrolysis, as summarised below.

Urea ($NH_2)_2CO$ yields 1.5 mol of $H_2$ through the thermal decomposition of the pure, crystalline compound into $N_2$ and $H_2$ via the intermediates ammonia and HCNO (isocyanic acid). In the presence of steam, hydrolysis of HCNO generates one additional mol of $NH_3$ which decomposes to a further 1.5 mol of $H_2$. The full reaction of urea with water therefore can yield a maximum of 3 mol of $H_2$ per mol of urea using a stoichiometric molar steam to carbon ratio (S:C) of 1.

Whereas the endothermic decomposition of pure crystalline urea to ammonia and isocyanic acid has been shown to occur without catalyst at moderate temperatures [17], and the exothermic catalytic hydrolysis of isocyanic acid proceeds at temperatures as low as 150 °C [14], the thermal decomposition (or 'cracking') of ammonia into $N_2$ and $H_2$ requires temperatures exceeding 450 °C for significant conversion in the presence of a catalyst.

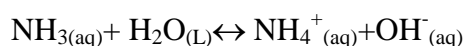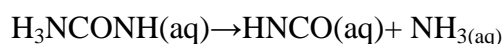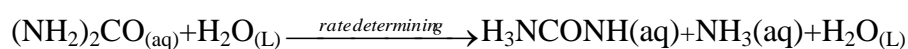Ammonia crackers commercialised as hydrogen generators rely on nickel based catalysts and operate at 850 °C. Hacker et al [18] investigated the activity of Pt-, Pd-, Ru-, and La$_2$O$_3$-doped Ni/Al$_2$O$_3$ catalysts in the ammonia cracking reaction. They found Ni/Ru-Al$_2$O$_3$ was the most active, allowing full ammonia conversion at 327 °C, compared to 427 °C for the un-doped Ni/Al$_2$O$_3$ catalyst. With the highest temperatures exceeding 450 °C for the ammonia cracking step, the reverse water gas shift reaction becomes active and thermodynamic equilibrium limits the yield of hydrogen, introducing CO in the gas product mixture. The chemical mechanism of H$_2$ production from crystalline urea and steam is described below:

Urea decomposition: $(NH_2)_2CO_{(S)} \xrightarrow{150–300^o C} HNCO_{(G)} + NH_{3(G)}$     $\Delta H^\circ{}_{298} = 186 kJ\ mol^{-1}$

Cyanic acid hydrolysis: $HNCO_{(G)} + H_2O \xrightarrow{T<150^o C} NH_{3(G)} + CO_2$     $\Delta H^\circ{}_{298} = -96\ kJ\ mol^{-1}$

Ammonia cracking: $2NH_{3(G)} \underset{Haber\ process, T<450^o C}{\overset{NH_3\ "cracking"\ T>450^o C}{\rightleftarrows}} N_{2(G)} + 3H_{2(G)}$     $\Delta H^\circ{}_{298} = 92.2\ kJ\ mol^{-1}$

Water gas shift:     $CO_2 + H_2 \leftrightarrow CO + H_2O$     $\Delta H^\circ{}_{298} = 41\ kJ\ mol^{-1}$

Overall, the complete, global reaction is mildly endothermic:

$(NH_2)_2CO_{(S)} + H_2O_{(G)} \rightarrow CO_2 + N_2 + 3H_2$     $\Delta H^\circ{}_{298} = 80.4\ kJ\ mol^{-1}$
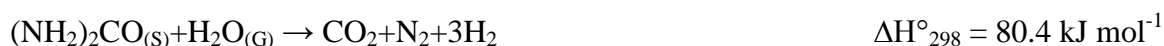
Alexandrova and Jorgensen found that in aqueous solution, urea yields ammonia and the H$_3$NCONH zwitterion intermediate via H-shuttling between the two amino groups by a neighbouring H$_2$O molecule in a rate determining step. The dissolved ammonia then equilibrates with ammonium ion (NH$_4{}^+$), with the H$_3$NCONH zwitterion undergoing a cis- to trans- conversion, followed by C-N bond cleavage, yielding a further ammonia molecule and isocyanic acid [19].

$(NH_2)_2CO_{(aq)} + H_2O_{(L)} \xrightarrow{rate\ determining} H_3NCONH(aq) + NH_3(aq) + H_2O_{(L)}$

$H_3NCONH(aq) \rightarrow HNCO(aq) + NH_{3(aq)}$

$NH_{3(aq)} + H_2O_{(L)} \leftrightarrow NH_4{}^+{}_{(aq)} + OH^-{}_{(aq)}$

$HCNO(aq) \leftrightarrow NCO^- + H^+$
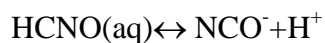
Mahalik et al investigated the instability of urea in aqueous solution as a function of urea concentration, stirring speed, and temperature [20]. With the urea conversion calculated on the basis of the measurement of the refractive index the urea-water solution, they found an Arrhenius rate constant $k=3.9 \times 10^6$ min$^{-1}$ exp(-7199/T) to be used with a first order rate equation. At 140 °C, a urea in water solution (10 to 40 wt%) converted by 50% in just under 3 min, but at ambient temperature, a 50 % conversion would require over 60 h.

In this study we propose urea as a hydrogen carrier which, as outlined earlier, has the potential to combine the qualities required for an excellent $H_2$ vector, and we report for the first time experiments on aqueous urea aimed at the production of hydrogen gas at the point of use. The compatibility of the reformate gas with proton exchange membrane fuel cells (PEMFC) is also considered.

## 2. Experimental

2.1. Thermodynamic calculations.

The feasibility of $H_2$ production of aqueous urea was investigated using thermodynamic calculations. The computation software EQUIL [21] was used, where the chemical species $CH_4$, $CO$, $CO_2$, $O_2$, $H_2O$, $H_2$, $N_2$, $NH_2$, $NH_3$, $CO(NH_2)_2$ (urea), HNCO and HCN were considered as potential equilibrium products. The calculations were performed over the temperature range 300-1280 K at atmospheric pressure and for molar steam to carbon ratios (S:C) from 0.25 to 7. The mol fraction of nitrogen of 0.631 was used to simulate the conditions of the experiments. The latter necessitated the use of $N_2$ dilution in order to reach closure of the elemental balances, and also helping reach the minimum gas flows required by the online analysers. Output values were tabulated at 10 K intervals for each

S:C ratio. Simulations of aqueous urea conversion to hydrogen as well as of ammonia decomposition were carried out in support of the discussion of experimental results.

2.2. Materials, experimental set-up and methods.

2.2.1. Materials

Urea (>99.5%) and de-ionized water was used in all the experiments. The catalyst was provided by Johnson Matthey, designed for the high pressures and temperatures of the methane steam reforming process, and contained 18 wt% NiO on a proprietary $Al_2O_3$ support. As received, it was in pellet form of 13.8 mm diameter and 18.4 mm long. The pellets were crushed and sieved to 0.66 - 1.70 mm size. Each experiment used undiluted 20 g of fresh catalyst. The bed occupied a height of 9 cm and volume of 7.9 $cm^3$ within the reactor tube and was supported on a stainless steel circular mesh screen. Reflecting the stringent conditions of its intended use as a catalyst developed many years of use in industry, the BET surface area of the as-received (oxidised) catalyst was just 3.262 $m^2$ $g^{-1}$, this would have the advantage of being less susceptible to loss of surface area caused by thermal sintering. Experiments using a bed of spherical $Al_2O_3$ pellets of ∼3 mm diameter (Sigma Aldrich) were also carried out to help determine the role of the Ni catalyst in the $H_2$ production mechanism. The amount used was chosen to offer the same bed volume as with the catalyst and resulted in a mass of alumina pellets of 10 g.

2.2.2. Experimental set-up

Figure 1 shows a schematic of the continuous down-flow packed-bed quartz reactor and its ancillary equipment. The reactor tube had an ID of 12 mm and was 70 cm long. It was connected at the top to a glass inlet section, and at the bottom to a glass outlet assembly and condensing system. The reactor was housed in a tube oven equipped with a programmable temperature controller that used the measurement of a type K thermocouple attached on the internal oven wall for control. Another type K thermocouple embedded in the catalyst was

7

used to measure the reactor bed temperature. MKS mass flow controllers ensured controlling the flows of $N_2$ and $H_2$ gases from BOC cylinders of >99.99% purity. Steel tubing (1 mm ID, 14 cm long) connected a syringe pump containing the urea-water mix to the inlet assembly. It then bent 90° downward via a Swagelok connector to a 2 mm ID injector. The injector ended 2 cm centrally above the top extremity of the reactor, perpendicular to the gas inlet.

2.2.3. Methods

A flow of 300 $cm^3 min^{-1}$(STP) of $N_2$ was used in all of the experiments. The system was at or near atmospheric pressure. The catalyst was reduced for 1 h at 500 °C by a flow of 30 $cm^3 min^{-1}$ (STP) of $H_2$ in 400 $cm^3 min^{-1}$ (STP) of $N_2$ prior to each experiment. The reactor was then purged with the same flow rate of $N_2$ for at least ten minutes. Aqueous urea with the desired steam to carbon ratio was then fed into the reactor via the syringe pump (New Era Pump Systems) at a constant rate of 10 ml $h^{-1}$ (20 °C). The condensate consisting mainly of un-reacted steam was then removed via two oil-cooled condensers and a silica gel trap. The condensate was collected immediately from a glass flask at the base of the outlet assembly, stored in glass vials and kept in dark refrigerated conditions at the end of each experiment prior to the $N_2$ purge to correspond to the conditions of steady state operation. This was then analysed for ammonium ion content. The ammonium ion's concentration in the condensates was measured using a Dionex DX-100 Ion Chromatograph at room temperature, with 0.02 mol methane sulphonic acid as eluent and Dionex polymeric packing (IONPAC CS12A), on a column 4 mm × 250 mm. Raw samples were diluted with deionised water to fit within the detection range of the analytical technique and were analysed at room temperature. pH was also determined for the condensates to ascertain that a correction for dissolved ammonia was not required. Indeed with measured pH all in the 9.9-11 region at room temperature, the condensates were not

expected to contain dissolved ammonia in any significant amount. Therefore the measured $NH_4^+$ by ion chromatography was taken to account for the full gaseous $NH_3$ product prior to condensing in water and ionising.

Hydrogen production experiments were performed on urea solutions at a set reactor temperature for the molar steam to carbon ratios (S:C) of 4, 5, 6 and 7:1. For the S:C of 4 and 5, the temperature of 600 °C was used. For S:C of 6 and 7, temperatures decreasing from 700 to 500 °C using 50 °C steps were used. Each new S:C ratio experiment required a fresh catalyst. Each $H_2$ production experiment ended with the system being purged with $N_2$ at the same flow rate and temperature to remove any residual gases. The $N_2$ purge ended when the residual gas concentrations returned to zero. Then, air at a rate of 1000 $cm^3$ $min^{-1}$ (STP) with a maximum temperature of 700 °C was fed to assess the accumulation of carbonaceous deposits in the reactor via the observation of the resulting oxidation to the products $CO_2$ and CO. Experiments with aqueous urea in the reactor loaded with $Al_2O_3$ pellets (in the absence of the Ni-catalyst, but using same bed volume) were carried out at S:C of 7 for temperatures between 500 and 700 °C with 50 °C increments, using the same feed conditions as those of the experiments with the Ni catalyst. This was to establish the contribution of the catalyst to the $H_2$ yield. Finally, experiments were also carried out with $NH_3$-water solutions using the same molar feed of 2H in the $NH_3$ as in the aqueous urea feed of the experiment with aqueous urea at S:C of 7, this was to aid the discussion of the $NH_3$ intermediate in the likely mechanism of hydrogen production when using aqueous urea. In this case, a commercial 35 wt% $NH_3$ solution was diluted with distilled water to the required amount and fed with the same syringe as with the urea experiments. The same reactor loading (20 g of Ni-catalyst) was also used and the temperatures of 500, 600 and 700 °C were chosen for the $NH_3$-water solutions catalytic cracking experiments. A final experiment of $NH_3$-water non-catalytic cracking at 600 °C was conducted with same feed

9

rate as the previous experiments with the catalyst, using a bed of $Al_2O_3$ pellets as described earlier (10 g, same volume as the catalytic experiments), to help discuss the contribution of the catalyst to the $H_2$ yield from $NH_3$ cracking.

A series of analysers from ABB Advance Optima carried out the online analysis of the dry reformate every 5 s. A non-dispersive infrared absorption module (Uras 14) monitored the CO, $CO_2$ and $CH_4$ dry vol% levels, a thermal conductivity analysis module (Caldos 15) measured $H_2$, and an ultraviolet absorption module (modified Limas 11) was used for the gaseous $NH_3$ analysis. The Uras 14 and Caldos 15 were non-sample destructive. During the air feed, a paramagnetic susceptibility module (Magnos 106) also by ABB Advance Optima, measured $O_2$ levels at the end of the line.

SEM images of the catalyst at 50kX magnification were taken with a Leo 1530 Field emission gun scanning electron microscope and saved in digital form using Smartsem v5 software.

Imaging and analysis of the catalyst's surface was also performed by TEM coupled with EDX. The equipment used for the catalysts tested was a FEI CM200 field emission gun (FEG) TEM running at 197 kV equipped with an Oxford Instruments energy dispersive X-ray (EDX) spectrometer and a Gatan Imaging Filter. The FEI Tecnai F20 microscope was fitted with a Gatan Orius SC600A camera and an Oxford Instruments INCA 350 EDX System with an 80 $mm^2$ X-Max SDD detector. Using an imaging filter, analysis of the crystal lattice spacing using Fast Fourier Transform (FFT) power spectra allowed deriving d-spacing values that, using library data, together with the EDX spectra, helped distinguishing between the $Al_2O_3$ support, the Ni and the NiO in the catalyst.

The surface of the as-received catalyst, of the catalyst after reduction under $H_2/N_2$ flow and on completion of the $H_2$ production experiments was characterised using $N_2$ adsorption-desorption isotherms and BET surface area obtained with a Nova® 2200 analyser made by

Quantachrome Instruments. The instrument was run in the 'classical' mode using helium as the carrier gas and nitrogen as the adsorbate. High purity gases were used, BOC CP Grade He and Zero Grade $N_2$.

X-ray diffraction (XRD) analysis was used to identify and quantify the relative amounts of different phases within the catalyst before and after the hydrogen production experiments. The model used for this work was an X'pert MPD by PANalytical with a copper k anode. A first set of scans was carried out on the samples using a range of angles from $2\theta=5°$ to $2\theta=90°$, at increments of $0.017°$, and scan step time of 40.7 s. The second set of scans was performed from $2\theta=20°$ to $2\theta=130°$, at increments of $0.017°$, and scan step time of 203.5 s. The 'Highscore Plus' software was used for peak fitting and analysis of the diffractograms. Quantification of the relative contributions of each component was achieved using Rietveld refinement [22]. The ICSD patterns used for the refinement were by Sawada [23] for alumina, Slack [24] for NiO and Swanson and Tatge [25] for Ni. The sizes of the Ni and NiO crystallites were obtained through the Highscore Plus software, which uses the pseudo-Voigt and Pearson VII profile functions to describe the peaks broadening and associated corrections (instrumentation and strain) in Scherrer's equation.

## 3. Results and Discussion

The reactants conversion fractions $x_{urea}$ and $x_{H2O}$, the selectivity to the hydrogen-containing products ($H_2$ SEL, $NH_3$ SEL, $CH_4$ SELH), the selectivity to the carbon-containing products ($CO_{SEL}$, $CO_2$ SEL and $CH_4$ SELC), and the hydrogen yield (mol rate $H_2$ produced/mol rate urea input) were calculated using materials balance spreadsheet developed in-house. These used as inputs (i) the molar input flow rates of urea and water calculated from the masses of urea and water in the feed solution, (ii) the syringe pump injection volume flow

rate, (iii) the measurements of the reactor effluent volume (mol) fractions of gaseous $H_2$, CO, $CO_2$, $CH_4$, and $NH_{3(v)}$ by the online gas analysers and (iv) the mol fraction of $NH_{3(l)}$ in the aqueous condensate from the $NH_4^+$ content measured by ion chromatography. The method for these calculations involved solving a system of three equations (N, C and H balances) with three unknowns (total dry gas molar outflow, urea and water molar outflows) is described in the appendix A1 (nomenclature) and A2 (calculation). For the aqueous ammonia cracking experiments, the assumption was made that water was not reacting (inflow=outflow) and this allowed the conversion of $NH_3$ to $H_2$, $H_2$ yield, and $H_2$ production rate to be calculated by solving the N and H elemental balances (appendix A3).

### 3.1. Equilibrium calculations

The calculated equilibrium hydrogen yield is shown in Fig. 2 in mol $H_2$ / mol urea. It exhibited a maximum for a given molar steam to carbon ratio which approached the maximum value of 3 corresponding to the complete conversion of urea and steam to $H_2$, $CO_2$ and $N_2$ as the steam to carbon ratio increased. The $H_2$ yield for S:C of 7 peaked at 2.85 mol $H_2$ / mol urea in the temperature range 547-597 °C, compared to 2.29 mol $H_2$ / mol urea at 707-717 °C for the stoichiometric ratio S:C of 1. High $H_2$ yields are obtained at high fuel and steam conversions coupled with high selectivity to $H_2$. The equilibrium calculations predicted complete fuel conversions ($x_{urea,eq}=1$) for all the conditions covered ($0 < T < 1000$ °C, $0.25 < S:C < 8$). The H-containing by-product $NH_3$ was not predicted to reach significant concentrations at equilibrium in the range of simulated conditions, with a maximum mol fraction of $NH_{3,eq}$ of $7.9 \times 10^{-4}$ obtained for S:C of 0.25 at 300 °C. HNCO was predicted with negligible concentrations at all conditions (mol fraction$<10^{-8}$). In contrast, $CH_4$ was the most significant H-containing by-product at temperatures below 330 °C for the whole S:C range studied, reflecting the dominance of the methanation reactions. Upon reaching higher temperatures the steam reforming of methane then became

12

responsible for $H_2$ starting to dominate the H-containing products. Accordingly, for a given S:C ratio, the $H_2$ yield underwent a steep rise from low but increasing temperatures (< 200-600 °C). After a peak in the $H_2$ yield, there was a subsequent slower decrease with further increases in temperature. The difference in gradients in $H_2$ yield with temperature on either sides of this peak could be explained by the medium endothermicity of the steam-urea to hydrogen reaction compared to the milder exothermicity of the water gas shift reaction (WGS), causing the reverse WGS reaction to become more favourable as temperature increases. This difference in gradient, compounded with Le Chatelier's principle which causes increasing hydrogen product yield with an increase in the reactant steam above stoichiometry, shifted the peak $H_2$ yield position towards lower temperatures as the S:C increased. To illustrate this, the calculated steam conversions for S:C from 0.25 to 8 are shown in Fig. 3 for temperatures between 330 and 1000 °C. They exhibited a peak which shifted to lower values and lower temperatures with increasing steam to carbon ratio above stoichiometry, following Le Chatelier's principle and its main effect on the equilibrium of the WGS. The $H_2$ yield and steam conversions shown in Figs. 2-3 indicated that the optimum temperatures for urea-steam conversion to hydrogen for S:C of 2 and above, were in the 500-620 °C range. In these conditions, the WGS reaction is more active than its reverse, as illustrated by $CO_2$ to CO ratios higher than 1, plotted in Fig. 4. The hydrogen production from urea with water at S:C at and above 2 and temperatures between 500 and 620 °C would therefore offer good conditions for carrying out sorption enhanced steam hydrogen production from aqueous urea by using the in-situ carbonation of a Ca-based sorbent, as demonstrated in previous investigations on crude glycerol and waste cooking oil [22,23]. This would avoid the need for separate high- and low-temperature WGS reactors, but would introduce a sorbent regeneration step. The latter would benefit from further integration such as that offered by the chemical looping process [27]. In-situ $CO_2$ capture as

a means of pre-combustion or post-combustion fuel decarbonisation is generating much interest in gasification and power generation applications.

3.2. Experiments of catalytic hydrogen production from aqueous urea solutions

The temperature range for the experiments was chosen as a compromise between the need to operate at the minimum required to activate the catalyst, reducing the energy costs of steam, while remaining as close as possible to the thermodynamically favourable conditions of maximum yield. Previous steam reforming work with the same catalyst using renewable alternative fuels such as glycerol [26] suggested that temperatures below 500 °C and steam to carbon ratios below 3 may lead to significant carbon deposition in the absence of $CO_2$ sorbent. Glycerol and urea have the same O/C ratio, where the O content is a strong indicator of significant coke formation on the catalyst. We therefore chose the temperature range of 550-700 °C for the experiments.

3.2.1 Effect of steam to carbon ratio on $H_2$ yield, reactant conversions and products distribution

The smallest steam to carbon ratio investigated in this study was determined by the solubility of urea in water at ambient temperature, while the highest aimed to avoid exaggerated steam raising costs, thus the range of S:C from 4 to 7 was used. Lower S:C ratios led to difficulties in fully dissolving urea in the water at the ambient laboratory temperature of ca. 20 °C.

The time-on-stream profiles of $H_2$, $CO_2$, CO and $CH_4$ concentrations in mol % in the dry gas for S:C of 6 at 600 °C are plotted in Fig. 5, with the calculated equilibrium values also plotted alongside for comparison. These profiles were typical of the other S:C ratios and temperatures investigated ($4 \leq$ S:C $\leq 7$ at 600 °C, $500 \leq T \leq 700$ °C for S:C of 6 and 7). They exhibited a fast rise to a steady-state, the latter revealing small oscillations in the $H_2$ profile but very stable $CO_2$, CO and $CH_4$ profiles. The conditions for these experiments

were very near equilibrium as shown by the closeness of the experimental profiles in Fig. 5 to the calculated equilibrium lines. Table 1 lists the $NH_4^+$ ion content in the condensate for each of the experiments measured by ion chromatography (in ppm mass basis). The dry syngas consisted of the main products $CO_2$ (4.6 mol %), $H_2$ (16 mol %), with hardly any of the undesired $CH_4$ and $NH_3$ by-products, little CO (1.4 mol %) due to the temperature of 600 °C and the equilibrium of the WGS reaction. The $N_2$ reaction product mixed with the $N_2$ carrier gas was found to be 77.9 mol % by balance to 100%. These concentrations, corrected for zero $N_2$ content, would become: $H_2$, 72.4%, $CO_2$, 20.8%, CO, 6.3%. The experimental and equilibrium calculations for urea and steam conversions, selectivity of the H- and C-containing products at steady-state, and the $H_2$ yield for the experiments at 600 °C and S:C from 4 to 7 are listed in Table 2. These outputs were close to the predicted equilibrium values for the range of conditions $5 \leq$ S:C $\leq 7$, with a trend towards conversions which, as expected from Le Chatelier's principle, were higher for urea and lower for steam as the S:C increased. The maximum $H_2$ yield was found, as expected from the equilibrium trends, at S:C of 7, with 2.57 mol $H_2$/ mol urea, which corresponded to 90% of the equilibrium value. The S:C of 7 corresponds to the commercial solution used in selective catalytic reduction of NO (AdBlue[TM] AUS32). The variations with S:C of the $H_2$ yield at steady state from Table 2 are also plotted in Fig. 6, revealing a decline in $H_2$ yield for S:C below 5. The causes of this decline can be found in the significant decrease in urea conversion from S:C of 5 compared to S:C of 4 ($x_{urea}$ of 0.95 vs. 0.88), while another contributing factor is the increase in $NH_3$ selectivity in the H-containing products (also plotted in Fig. 6), caused by the increased concentration of ammonium ion measured in the reformer condensate. This would indicate the difficulty of the catalyst to dissociate (crack) the ammonia at lower steam to carbon ratios and suggests that optimisation of the catalyst in this respect would be beneficial. It can be observed that the only other H-containing by-

15

product $CH_4$ did not appear significantly dependent on the steam to carbon ratio, as predicted by the equilibrium calculations.

### 3.2.2. Effect of temperature on outputs

The process outputs' dependence on temperature can be seen in Table 3 for S:C of 7 at temperatures from 500 to 700 °C with 50 °C steps. The effects of temperature in the range 500-700 °C on the process outputs were much larger than those observed when the S:C varied from 7 down to 4 at 600 °C. Firstly, the fraction of urea converted evolved from a near complete conversion at 600 °C to the poor value of 0.51 at 500 °C, with very significant drops observed between 600 and 550 °C, and again between 550 and 500 °C. This was caused by a decrease in catalyst activity in the urea steam reaction below 600 °C, as observed in previous studies of steam reforming that used the same catalyst with other types of feedstock (glycerol [26], and waste cooking vegetable oil [27]). In this temperature region, the steam conversion was expected from equilibrium point of view to increase imperceptibly for temperature decreasing from 700 to 500 °C. The general trend of the experiments also showed a slight increase in steam conversion from 0.08 to 0.13 in the same temperature range (Table 3), although the experiment at 550 °C indicated a larger deviation from equilibrium with a poorer than expected steam conversion (0.08 vs. 0.12). Regarding the temperature dependence of the selectivity to the H-containing products, the selectivity to $CH_4$ was insignificant (0 % to 0.2% with decreasing temperature), as opposed to the selectivity to $NH_3$, which increased very significantly from 2.6% to 23.8% between 550 and 500 °C, in contrast to the small equilibrium values. This indicated that the catalyst's ability to dissociate $NH_3$ was significantly affected between 500 and 550 °C, providing another opportunity for catalyst optimisation for this process. Not shown is the negligible contribution that the $NH_3$ in the dry gases made to the overall $NH_3$ selectivity, indicating that more than 99.3% of the $NH_3$ generated was collected in the condensate.

16

Accordingly, the larger selectivity to $NH_3$ adversely affected the selectivity to $H_2$, causing a corresponding significant drop from 97.1% to 76% between 550 and 500 °C. However, above 550 °C, the selectivity to $H_2$ remained very high, reaching above 99.6% from 650 °C. The selectivity to the carbon-containing products followed closely their equilibrium calculated counterpart in the temperature range 500-600 °C, and, as $CH_4$ was near non-detectable, the selectivity to $CO_2$ and CO reflected the increasingly active reverse water gas shift reaction with increasing temperature, as discussed earlier on the basis of Fig. 4. The $H_2$ yield exhibited a plateau with temperature above 600 °C. It showed a maximum and closest value to equilibrium at 700 °C, reaching 95% of its equilibrium value (2.63 mol $H_2$/mol urea compared to 2.78). This plateau can be seen more clearly in Fig. 7, where the $H_2$ yield variations with temperature for the two S:C of 6 and 7 are plotted. The $H_2$ yield-temperature profiles in Fig. 7 indicate that the plateau is repeatable for the two S:C sets of experiments. The effect of temperature on the $H_2$ yield is the result of the effects on the urea and steam conversions, and on the selectivity to $H_2$. Figure 7 also includes the temperature dependent variations of the selectivity of $NH_3$ from the H-containing products ($H_2$, $CH_4$ and $NH_3$) for S:C of 6 and 7. It is clear that they exhibited the inverse trends to the $H_2$ yield, resulting in the same plateau effect, but reversed. As indicated in the experimental section, a fresh catalyst was used for each S:C ratio investigated.

3.3 Experiments of non-catalytic hydrogen production from aqueous urea

Table 4 reports the process outputs for the hydrogen production from aqueous urea experiments at S:C of 7, carried out on the bed of $Al_2O_3$ pellets, in the absence of the Ni-catalyst, for the temperature range 500-700 °C. As the volume occupied by the $Al_2O_3$ pellets was the same as that of the experiments with the Ni catalyst, and given that the same feed rates were used at S:C ratio of 7 and for the same temperatures range, it was assumed that the residence time for the two experiments would be roughly similar, allowing the

contribution of the Ni catalyst to the $H_2$ yield to be estimated. These experiments revealed very little conversion of the urea to the CO, $CO_2$ and $CH_4$ products (average of 0.29) when the equivalent experiments with the Ni catalyst exceeded 0.97 at and above 600 ℃. Accordingly, the $H_2$ yield during the experiments on $Al_2O_3$ pellets was below 0.06 mol/mol urea, in contrast to the values above 2.6 found with the use of the Ni catalyst at and above 600 ℃. Considering the selectivity to the H-products, the experiments on $Al_2O_3$ revealed the largest selectivity to the $NH_3$ by-product (around 90%), which was calculated based on the very large concentrations of ammonium ion measured in the condensates (above 86 000 ppm mass, Table 4). The carbon products were dominated by the $CO_2$ gas, with selectivity in excess of 89%. These experiments resulted in white sticky residues that adhered to the condenser wall and ended obstructing the reactor's effluents, unlike the experiments with the Ni-catalyst, which remained very stable. The conclusions from this set of experiments were that non-catalytic hydrogen production from aqueous urea is not a feasible process and that the results near equilibrium obtained with the use of the Ni bed material are attributable to the catalytic activity of the Ni. The $Al_2O_3$ had some activity in converting the urea to $CO_2$ but hardly any activity in ammonia cracking (which will be further evidenced in the next section).

3.4 Experiments of catalytic and non catalytic $NH_3$ cracking in water solution

The decomposition of $NH_3$ into $0.5N_2$ and $1.5H_2$ by thermal catalytic treatment ('ammnonia cracking') is expected to be the final step of the conversion of aqueous urea into hydrogen, following the initial decomposition of urea into isocyanic acid and ammonia, and the hydrolysis of the isocyanic acid into further ammonia and carbon dioxide. As seen in the introduction, the reaction of ammonia catalytic cracking requires temperatures above 450 ℃, and commercial ammonia crackers typically operate at 800 ℃ with Ni catalysts.

18

Ammonia cracking experiments were carried out in the present study on the Ni catalyst using same feed rates, on a (2H) basis in the non-water reactant ($NH_3$ or urea), but also same reactor loading, and using the same temperature range as in the experiments with aqueous urea at S:C of 7 reported in section 3.2. The results are reported in Table 5 for the three temperatures 500, 600 and 700 °C. An additional experiment at 600 °C is also reported, which used a bed of alumina pellets of same volume as the catalyst, similarly to the experiments reported in section 3.3. Comparisons are presented with the equilibrium calculation for the same conditions. From the stoichiometry of the reaction the maximum yield of hydrogen is 1.5 mol $H_2$/ mol $NH_3$. First of all, the experiment on $Al_2O_3$ pellets at 600 °C exhibited a negligible hydrogen yield (0.08 mol $H_2$/ mol $NH_3$), therefore there was little evidence of ammonia cracking by non-catalytic means. In contrast, at the same temperature and in the presence of the Ni catalyst, the $H_2$ yield was the highest of the temperature range (500-700 °C) with a significant $NH_3$ conversion to $H_2$ of 0.7, ie. 70% of the predicted equilibrium value, corresponding to a $H_2$ yield of 1.05 mol/mol $NH_3$. This was lower than the equivalent aqueous urea experiment, which had attained 90 % of the predicted equilibrium $H_2$ yield (Table 3). A comparison in the weight hourly space velocity (WHSV) of the two experiments showed that the ammonia cracking experiment (at 1.16 h$^-$$^1$) had even benefitted from a slightly higher residence time than the urea experiment (1.6 h$^-$$^1$). Thus its larger gap to equilibrium could not be attributed to less contact time with the catalyst. However this tendency of the urea-water reaction to approach closer to equilibrium in a shorter residence time than the $NH_3$ cracking reaction of same (2H) non-water feed is in agreement with the difference found between the 'ΔG' (change in Gibbs function) at 600 °C for the urea-water reaction (-22.6 kJ/mol mixture) and for the ammonia cracking reaction (-12.1 kJ/mol mixture). The more negative ΔG for the urea-water mixture indicated a more thermodynamically favourable reaction than the ammonia cracking experiment.

19

This would support the fact that the mechanism of $H_2$ production from aqueous urea water is more active than just a sequence of decomposition to HNCO and $NH_3$, followed by hydrolysis of HNCO and finally by ammonia cracking, and that it could be defined on its own, much like a complete steam reforming reaction. The difference in conversion to hydrogen between the ammonia-water and the urea-water solutions became more marked at 700 °C. At this temperature, the aqueous urea experiment had a $H_2$ yield that was 95% close to the equilibrium value (Table 3), whereas the ammonia cracking experiment was just 59% from the equilibrium value (table 5). At 500 °C, the gap between experiment and equilibrium, as expressed by the ratio of $H_2$ yield to equilibrium yield, was found to be about the same for the ammonia cracking as for the aqueous urea experiments (value of 0.47), supporting the earlier finding that the Ni catalyst was not very active at this temperature (Fig. 7). To conclude this part of the study, it would seem that operating at 600 °C would offer the most benefits given the higher equilibrium $H_2$ yield that can be achieved and the good performance of the catalyst in both aqueous urea conversion and ammonia cracking. This temperature would also be most suited to the sorption enhanced process using a CaO-based $CO_2$ sorbent material, which would eliminate the carbon containing gases from the product, leaving just a 75 / 25 vol.% $H_2/N_2$ mixture.

3.5 Catalyst characterisation

3.5.1 Surface analysis

SEM images taken of the catalyst before and after the experiments at S:C of 6 are shown in Fig. 8. The images were taken on the catalyst following the experiment at 500 °C, and before regeneration or reduction steps by air and $H_2/N_2$ flow. Thus, the conditions corresponded to a poor urea and steam conversion fraction (0.52 and 0.15 respectively), with large excess of steam in the reactor and very significant $NH_3$ production ($SEL_{NH3}$ of 20.1%). Despite these adverse conditions, the images indicated no obvious morphological

changes in the larger crystallites structure ($Al_2O_3$), although dispersed particulates of around 50 nm size are visible on the surface of the large crystallites on the used catalyst in Fig. 8. There were no carbonaceous deposits, a result supported by the EDX spectra which revealed only the presence of the Ni, Al and O elements (not shown), expected of a clean catalyst.

The surface of the unused catalyst, the catalyst reduced under $H_2/N_2$ flow, and after completion of the experiments of hydrogen production from aqueous urea was analysed using $N_2$ adsorption and desorption isotherms. All of the isotherms were of type II according to BDDT classification [28], indicating that the catalyst had little porosity. The lack of porosity in the catalyst was confirmed by the low values obtained from the BET surface area measurements, between 2.3 and 3.7 $m^2$ $g^{-1}$ for the three catalysts samples, and corroborated by the electron microscopy images. As physical adsorption/ desorption isotherms are most useful in the range of 2-20 nm [28] the isotherms were not analysed for pore size distributions. The measured BET areas for the three catalyst samples are listed in Table 6.

3.5.2. Materials phases present in the catalyst and crystallite sizes

Identification of the crystalline phases present in the catalyst at the different stages of the experiment (unused, $H_2$-reduced, after experiments of $H_2$ production from aqueous urea) was attempted by TEM-EDX coupled with FFT of the power spectra from the images, and by Rietveld refinement [22] performed on the powder XRD spectra, as described in the experimental methods section. This aimed at assessing the degree of catalyst deactivation induced by the experiments of hydrogen production from aqueous urea in the form of the catalytically inert nickel oxide phase and the possible presence of carbon deposits. For the sake of succinctness, a TEM image and EDX spectrum are shown only for the catalyst after the aqueous urea conversion experiments. The TEM images of the unused catalyst revealed

the smooth surface of the alumina support with dispersed particles of the catalyst, of size exceeding 50 nm, with the EDX spectra from the particles revealing large peaks for the Ni and O elements. The crystallites size derived from the XRD peaks indicated 53.9 nm for the NiO in the as-received catalyst, in agreement with the TEM images. Table 6 lists the sample phases composition calculated with Rietveld refinement from the two sets of XRD spectra obtained for the three samples as-received, $H_2$-reduced and after the aqueous urea conversion experiments.

 Rietveld refinement on the two Powder XRD spectra obtained from the same as-received catalyst sample revealed a composition of 18.0 wt % NiO with 82.0 wt% $Al_2O_3$ from the first spectrum, and no other crystalline phases present, and 17.7 wt% NiO with 82.3 wt% of $Al_2O_3$ from the second spectrum. Both measurements very close to the expected composition provided by the manufacturer (JM), thus instilling high confidence in the Rietveld refinement technique for the quantification of NiO and $Al_2O_3$ in the sample.

TEM on the catalyst after reduction under $H_2/N_2$ flow indicated a similar particle-support morphology as the unused catalyst, with the EDX on the catalyst revealing large peaks for the nickel element, but also visible were very minor peaks of Al and O, where the latter could have originated either from the $Al_2O_3$ support, especially since Al was also present, or small amounts of NiO. The Ni crystallite size derived from XRD was 19 nm. Rietveld refinement on the two spectra obtained from the $H_2$-reduced catalyst quantified NiO at 1.6 and 0 wt% respectively, with the balance as metallic Ni, indicating a nearly fully reduced state.

TEM on the catalyst after the set of aqueous urea conversion experiments, which ended with the conditions of S:C of 5 at 500 °C, revealed a similar morphology of particles distributed on the support. This is shown in Fig. 9, where two areas were focussed-on for the measurement of the FFT's lattice fringes inter-planar spaces (d-spacing). EDX on the

used catalyst was also similar to that of the reduced catalyst, with only Ni, Al and O, and no detectable carbon. The measured d-spacing values of 0.19 and 0.24 nm were attributable to Ni [29] and NiO [30]. The use of d-spacing values alone to try to differentiate between Ni and NiO is limited given their closeness, but in combination with EDX spectra focussed on the particles with very little oxygen, can confirm the d-spacing for Ni as opposed to NiO. The catalyst after the experiments exhibited Ni and NiO crystallite size of 52.0 nm and 51.0 nm respectively derived from XRD. Rietveld refinement carried out on the two spectra obtained from the same sample indicated that the used catalyst contained 2.7 and 3.0 wt% NiO respectively, with no other oxides of nickel being identified. The goodness of fit in the Rietveld refinement for the first sample is shown in Fig. 10 where the residual between observed spectrum and modelled spectra using Rietveld refinement is plotted. Although not zero over the whole spectrum, the residual was typically less than 10% of the observed peaks' height. The robustness of application of the Rietveld refinement technique's to these samples (unused, reduced, after experiments) was further assessed by checking the elemental balance from one catalyst state to the next. This was done on the assumption that neither the aluminium nor the nickel elemental contents in the samples were expected to change as the catalyst went from its unused condition (fully oxidised) to its final used state. For the two batches of spectra obtained for each condition, an elemental balance on Al, Ni and O was performed, and errors calculated for each element. These calculations revealed, assuming accurate unused catalyst composition, that the Al balance deviated for the subsequent states by a maximum of 6.5%, and in average 5%, while the O balance deviated by a maximum of 5.9%, and in average 3.6%. The Ni balance deviated by a maximum of 10.6%, and in average 9.2%. This validity check reveals that the Rietveld refinement could be improved on the quantification of Ni, as confirmed in Fig. 10 by the residual between the observed and modelled spectra. However, overall the derived results were deemed

worthy of confidence, in particular as the two compositions derived from the unused catalyst were so close to the expected 18 wt% $NiO/Al_2O_3$. Thus, the low amount of NiO in the catalyst after the aqueous urea conversion experiments, calculated from the Rietveld refinement, was a surprising and desirable outcome, since NiO does not exhibit steam reforming activity with common hydrocarbon fuels, in contrast to metallic Ni. The crystallite sizes derived from XRD for the catalyst as received, reduced, and post-experiments, were consistent with the particulate sizes visible on the TEM images attributed to Ni and NiO, and support the finding that little sintering by particle diffusion and growth had occurred as a result of the experiments.

Considering in combination the materials characterisation outputs (SEM/TEM images, EDX spectra, FFT d-spacing values on the catalyst particles, Rietveld refinement of powder XRD spectra), the used catalyst emerged little affected in terms of surface morphology, and remained carbon and almost nickel-oxide free after the experiments. These were conducted at relatively low reaction temperatures, sometimes leading to incomplete fuel conversion, thus there was a high expectation of carbon deposition. In addition they were carried out in large excess of steam, which was expected to cause a net formation of NiO by water splitting on the Ni catalyst. The characterisation of the bed material thus indicated a robust catalyst for the conversion of aqueous urea to hydrogen. It is anticipated that the selectivity to ammonia would decrease in favour of the desired product hydrogen when using a material exhibiting a higher surface area and lower Ni crystallites size, but offering a similar resistance to coking and NiO formation under the same aqueous urea experimental conditions as the present work. Future studies will endeavour to test such catalysts for higher activity in ammonia cracking and expected improvement on the $H_2$ yield. Another optimisation of the process of producing hydrogen from aqueous urea will include exploring the feasibility of sorption enhancement. The in-situ capture of the $CO_2$ from the

syngas in the reformer would be expected to extend the range of optimum conditions towards lower temperatures and lower steam to carbon ratios and overcome the limitations of thermodynamic gas equilibrium. The resulting dry syngas with complete $CO_2$ capture would then be close to the ideal composition of 75% mol $H_2$ and 25 mol% mol of $N_2$. As proton exchange membrane fuel cells (PEMFC) have been found not to be adversely affected by this level of dilution of $N_2$ [31], the sorption enhanced process could connect almost directly to the PEMFC, without the need for high and low temperature shift reactors.

## 4. Conclusions

Thermodynamic calculations showed there is an optimum temperature range for the conversion of urea and steam between 500 and 620 °C to produce $H_2$, $CO_2$ and $N_2$ that is caused by the juxtaposition of the relatively mild endothermic of the urea-water reaction with the weak exothermicity of the water gas shift reaction. Combining this theoretical temperature range with the need to minimise the energy cost of raising steam and operate with an active catalyst resulted in optimum experimental conditions for hydrogen production from aqueous urea of around 600 °C with steam to carbon ratios between 5 and 7. For temperatures above 550 °C the urea conversion and $H_2$ yield increased to close to the equilibrium values (near 3 mol $H_2$/mol urea or 10.07 wt% urea) to the detriment of the undesirable ammonia by-product. The $H_2$ production was shown to be attributable to catalytic reactions as opposed to thermal process, via a mechanism that is more active than the 3-step reaction process described in the literature (urea decomposition to HNCO and $NH_3$, HNCO hydrolysis to $NH_3$ and $CO_2$, and $NH_3$ cracking). The catalyst did not exhibit the expected symptoms of deactivation by either carbon deposition, increase in crystallite

size or surface area, or conversion of the Ni to NiO, as evidenced by SEM/TEM-EDX, FFT d-spacing values, $N_2$ adsorption/desorption, Rietveld refinement of powder XRD spectra.

## Appendix

### A1 Nomenclature:

$t$    duration of experiment, (s).

$dt$  sampling interval, (s).

$\dot{n}, \dot{n}_i$  total molar flow rate and molar flow rate of species $i$ at time $t$, (mol s$^{-1}$).

$y_i$ mol fraction of i in the dry gas, (known from online gas measurements)

$y'_{NH3}$ liquid mol fraction of $NH_3$ in the condensate (known from ion chromatography measurement)

$cond$ subscript relevant to condensate

$in, out$   subscript relevant to (known) flows entering or (unknown) flows leaving the reactor.

$\dot{n}_{NH_3,c,out}$   molar flowrate of $NH_3$ leaving the reactor in the condensate (unknown)

$dry$   conditions after condensate trap, prior to dry gas analyses.

$C_nH_mO_kN_j$  molar elemental formula of the fuel (known)

$n$, $m$, $k$, and $j$   moles of C, H, O and N in the fuel ($C_nH_mO_kN_j$), for urea, $n=1$, $m=4$, $k=1$

## A2 Equations for the reactant conversions, selectivity to products and $H_2$ yield from aqueous urea solutions using elemental balances:

$$\dot{n}_{cond} = \dot{n}_{H_2O,out} + \dot{n}_{NH_3,c,out}$$

$$\dot{n}_{NH_3,c,out} = y'_{NH_3} \times \dot{n}_{cond}$$

$$\Rightarrow \dot{n}_{NH_3,c,out} = \left( \frac{y'_{NH_3}}{1 - y'_{NH_3}} \right) \dot{n}_{H_2O,out} \quad \text{Eq.1}$$

The elemental balance equations are presented below with the three unknown terms on the *LHS* (molar output flow rates of dry gas, unreacted water and unreacted fuel $C_nH_mO_kN_j$ where, for urea, $n=1$, $m=4$, $k=1$ and $n=2$) and the known terms (reactant input molar flow rates) on the *RHS*.

From the nitrogen elemental balance:

$$\left(2y_{N_2} + y_{NH_3}\right) \times \dot{n}_{out,dry} + \left( \frac{y'_{NH_3}}{1 - y'_{NH_3}} \right) \times \dot{n}_{H_2O,out} + j \times \dot{n}_{CnHmOkNj,out} = j \times \dot{n}_{CnHmOkNj,in} + 2\dot{n}_{N_2,in} \quad \text{Eq.2}$$

From the carbon elemental balance:

$$\left( \frac{\left(y_{CO} + y_{CO_2} + y_{CH_4}\right)}{n} \times \dot{n}_{out,dry} \right) + 0 \times \dot{n}_{H_2O,out} + 1 \times \dot{n}_{CnHmOkNj,out} = \dot{n}_{CnHmOkNj,in} \quad \text{Eq.3}$$

From the hydrogen elemental balance:

$$\left(4y_{CH_4} + 2y_{H_2} + 3y_{NH_3}\right) \times \dot{n}_{out,dry} + \left(2 + \frac{3y'_{NH_3}}{\left(1 - y'_{NH_3}\right)}\right) \times \dot{n}_{H2O,out} + m \times \dot{n}_{CnHmOkNj,out}$$

$$= m \times \dot{n}_{CnHmOkNj,in} + 2\dot{n}_{H2O,in} \quad \text{Eq.4}$$

The system of three independent equations Eqs 2-4 and 3 unknowns is solved using the determinants method in an excel spreadsheet. With the unknowns now solved, the reactant conversions are:

$$x_{CnHmOkNj} = \frac{\dot{n}_{CnHmOkNj,in} - \dot{n}_{CnHmOkNj,out}}{\dot{n}_{CnHmOkNj,in}} \quad \text{Eq.5}, \quad x_{H_2O} = \frac{\left(\dot{n}_{H_2O,in} - \dot{n}_{H_2O,out}\right)}{\dot{n}_{H_2O,in}} \quad \text{Eq.6}$$

Rates of products evolution from the reformer in mol s$^{-1}$:

$$\dot{n}_{H_2,out} = y_{H_2} \times \dot{n}_{out,dry}, \quad \dot{n}_{CO_2,out} = y_{CO_2} \times \dot{n}_{out,dry}, \quad \dot{n}_{CO,out} = y_{CO} \times \dot{n}_{out,dry},$$

$$\dot{n}_{CH_4,out} = y_{CH_4} \times \dot{n}_{out,dry},$$

$$\dot{n}_{NH_3,out} = y_{NH_3} \times \dot{n}_{out,dry} + \left( \frac{y'_{NH_3}}{1 - y'_{NH_3}} \right) \times \dot{n}_{H_2O,out} \quad \text{Eqs.7 - 11}$$

Selectivity of H-containing products in %:

$$SEL_{H_2} = 100 \times \frac{\dot{n}_{H_2,out}}{\dot{n}_{H_2,out} + \dot{n}_{NH_3,out} + \dot{n}_{CH_4,out}}, \quad SEL_{NH_3} = 100 \times \frac{\dot{n}_{NH_3,out}}{\dot{n}_{H_2,out} + \dot{n}_{NH_3,out} + \dot{n}_{CH_4,out}},$$

$$SELH_{CH_4} = 100 \times \frac{\dot{n}_{CH_4,out}}{\dot{n}_{H_2,out} + \dot{n}_{NH_3,out} + \dot{n}_{CH_4,out}} \quad \text{Eqs.12-14}$$

Selectivity of C-containing products in %:

$$SEL_{CO_2} = 100 \times \frac{\dot{n}_{CO_2,out}}{\dot{n}_{CO_2,out} + \dot{n}_{CO,out} + \dot{n}_{CH_4,out}}, \quad SEL_{CO} = 100 \times \frac{\dot{n}_{CO,out}}{\dot{n}_{CO_2,out} + \dot{n}_{CO,out} + \dot{n}_{CH_4,out}},$$

$$SEL_{CH_4} = 100 \times \frac{\dot{n}_{CH_4,out}}{\dot{n}_{CO_2,out} + \dot{n}_{CO,out} + \dot{n}_{CH_4,out}} \quad \text{Eqs.15-17}$$

$$H_2 \, yield = \frac{\dot{n}_{H_2,out}}{\dot{n}_{CnHmOkNj,in}} \quad \text{mol s}^{-1} \, H_2 \, \text{per mol s}^{-1} \, \text{fuel}$$

$$or \quad \frac{2 \times \dot{n}_{H_2,out}}{(12n + m + 16k) \times \dot{n}_{CnHmOkNj,in}} \quad \text{in wt\% of fuel} \quad \text{Eq.18}$$

**A3 Equations for the reactant conversions, selectivity to products and H₂ yield from ammonia-water solutions using elemental balances**:

For ammonia 'fuel', we use a special case of the equations in A2 for which $n$ and $k$ in the fuel $C_nH_mO_kN_j$ are set to zero, j=1 and m=3. Only the N and H-balances (Eqs. 2,4) are used, eliminating of the outflow of water as an unknown since it is assumed not to react ( $\dot{n}_{H_2O,out} = \dot{n}_{H_2O,in}$ ).

## References

[1] A. N. Rollinson, J.M. Jones, V. Dupont and M.V. Twigg, Energy Environ. Sci., 4(2011) 1216-1224.

[2] S. Satyapol, J. Petrovic, C. Read, G. Thomas, G. Ordaz, Catal. Today 120 (2007) 246-256.

[3] M.A. Singer, Comp. Biochem.Physiol., Part B: Biochem. Mol. Biol. 134 (2003), 543-558.

[4] M.S. Thirkildsen, G.M. King, B.A. Lomstein, Aquat. Microb. Ecol. 10 (1996) 173-179.

[5] T.D. Chadwick, P.A. Wright, J. Exp. Biol. 19 (1999) 2653–2662.

[6] P.J. Walsh, M.J. Heitz, C.E. Campbell, G. Cooper, M. Medina, Y. Wang, G. Goss, V. Vincek, C. Wood, C. Smith, J. Exp. Biol. 203 (2000), 2357–2364.

[7] C.A. Miller, P.M. Glibert, J. Plankton Res. 20 (1998), 1767-1780.

[8] S. Kojima, A. Bohner, N. Von Wirén, J. Membr. Biol. 212 (2006) 83-91.

[9] United Nations International Register of Potentially Toxic Chemical, Organisation for Co-operation and Development Screening Dataset, Urea 57-13-6; United Nations Publications: Geneva, 1996; pp 1-121.

[10] M. Maurer, W. Pronk, T.A. Larsen, Water Res. 40 (2006) 3153-3166.

[11] J. Hanæus, D. Hellstrom, E. Johanson, Water Sci. Technol. 35 (1997), pp.153-160.

[12] B. Elvers, B. and S. Hawkins, Ullman's Encyclopedia of Industrial Chemistry (5th ed) A27 Thorium and Thorium Compounds to Vitamins; Wiley-VCH: Weinheim, 1996; pp 333-365.

[13] P. Heffer, M. Prud'homme, International Fertilizer Industry Association 76th Annual Conference, Vienna (Austria) 19-21 May 2008. Medium-term Outlook for Global Fertilizer Demands, Supply and Trade 2008 – 2012 Summary Report; IFA: Paris, 2008, 7.

[14] S.D. Yim, S.J. Kim, J.H. Biak, I-S Nam, Y.S. Mok, J-H Lee, B.K. Cho, S.H. Oh, Ind. Eng. Chem. Res. 43 (2004), 4856-4863.

[15] S. Fable, F. Kamakaté, S. Venkatesh. Selective Catalytic Reduction Urea Infrastructure Study 2002. NREL/SR-540-32689; National Renewable Energy Laboratory: California, 2002, 2.1-2.5.

[16] W.R. Epperly, Chem. Technol. 21 (1991) 429-431.

[17] A. Lundström, B. Andersson, L. Olsson, Chem. Eng. J. 150(2009) 544-550

[18] V. Hacker and K. Kordesch. *Handbook of Fuel Cells – Fundamentals, Technology and Applications.* Volume 3, Part 2, pp 121–127. Edited by Wolf Vielstich, Arnold Lamm, Hubert A. Gasteiger, John Wiley 2003.

[19] A. N. Alexandrova and W. L. Jorgensen, J. Phys. Chem. B,111 (2007), 720-730

[20] K. Mahalika, J.N. Sahua, A.V. Patwardhand, B.C. Meikapa, J. Hazard. Mater. 175 (2010) 629–637

[21] A.E. Lutz, F.M. Rupley, R.J. Kee, EQUIL: a Program for Computing Chemical Equilibria. CHEMKIN Collection, Release 3.5; Reaction Design, Inc: San Diego, 1999; pp 2-20.

[22] L.B. McCusker, R.B. Von Dreele, D.E. Cox, D. Louër and P. Scardi, J. Appl. Crystallogr. 32 (1999) 36-50.

[23] H, Sawada, Mater. Res. Bull., 29 (1994) 127-133

[24] G. A. Slack, J. Appl. Phys., 31 (1960) 1571-1582

[25] H.E. Swanson and E. Tatge, *Standard X-Ray Diffraction Patterns* Vol 1 National Bureau of Standards (U.S) circ 539, (1953)

[26] B. Dou, G.L. Rickett, V. Dupont, P.T. Williams, H. Chen, Y. Ding, M. Ghadiri, Bioresour. Technol. 101 (2010) 2436-2442.

[27] P. Pimenidou, G. L. Rickett, V. Dupont, M. V. Twigg, Bioresour. Technol. 101 (2010) 9279–9286.

[28] S. Lowell, J. E. Shields, Powder Surface Area and Porosity, second edition, Chapman and Hall, 1984 ISBN 9780412252402

[29] A.W. Hull, Phys. Rev., Vol 17, Issue 5 (1921) 571-588.

[30] S. Wies. and W.S.L.Eysel, Institut der Universitaet Heidelberg, Germany. ICDD Grand-in-Aid, Mineral Petrograph.

[31] S. Kim, J.W. Shimpalee, J.W. Van Zee, J. Power Sources Vol 137 (2004) 43-52.

**Table 1** Ammonium ion content in the condensates (in ppm, mass basis) for all the experiments with aqueous urea on the Ni catalyst.

| Temp (°C) | S:C=7 | S:C=6 | S:C=5 | S:C=4 |
|-----------|-------|-------|-------|-------|
| 700 | 127 | 1689 | _ | _ |
| 650 | 1928 | 4029 | _ | _ |
| 600 | 7368 | 15315 | 15488 | 28252 |
| 550 | 8232 | 25129 | _ | _ |
| 500 | 65493 | 71213 | _ | _ |

**Table 2** Mean experimental and calculated equilibrium reactant conversions and products distribution at 600 $^o$C for urea reactant using the Ni catalyst.

| S:C | | $x_{urea}$ | $x_{H2O}$ | Sel. H-products % | | | Sel. C-products % | | | $H_2$ Yield |
|-----|---|-----------|-----------|-------|--------|--------|--------|------|--------|-------------|
| | | | | $H_2$ | $NH_3$ | $CH_4$ | $CO_2$ | CO | $CH_4$ | mol/mol urea |
| 4 | Exp | 0.88 | 0.15 | 95.3 | 4.38 | 0.32 | 73.8 | 25.4 | 0.01 | 2.17 |
| | Eq. Calc | 1.00 | 0.19 | 99.5 | 0.05 | 0.42 | 75.5 | 23.4 | 1.14 | 2.72 |
| 5 | Exp | 0.95 | 0.15 | 97.0 | 2.65 | 0.32 | 74.5 | 24.6 | 0.01 | 2.53 |
| | Eq. Calc | 1.00 | 0.16 | 99.8 | 0.05 | 0.20 | 80.1 | 19.4 | 0.56 | 2.78 |
| 6 | Exp | 0.93 | 0.13 | 96.6 | 3.24 | 0.18 | 76.3 | 23.2 | 0.01 | 2.50 |
| | Eq. Calc | 1.00 | 0.14 | 99.8 | 0.04 | 0.12 | 82.8 | 16.8 | 0.32 | 2.82 |
| 7 | Exp | 0.97 | 0.10 | 98.0 | 1.92 | 0.05 | 80.6 | 19.2 | <0.01 | 2.57 |
| | Eq. Calc | 1.00 | 0.12 | 100 | 0.04 | 0.07 | 85.3 | 14.5 | 0.19 | 2.85 |

**Table 3** Mean experimental (Exp) and calculated equilibrium (Eq.Calc) reactant conversions and products distribution for urea reactant at S:C = 7 using the Ni catalyst.

| Temp °C | | $x_{urea}$ | $x_{H2O}$ | Sel. H-products % | | | Sel. C-products % | | | $H_2$ Yield mol/mol urea |
|---|---|---|---|---|---|---|---|---|---|---|
| | | | | $H_2$ | $NH_3$ | $CH_4$ | $CO_2$ | CO | $CH_4$ | |
| 500 | Exp | 0.51 | 0.13 | 76.0 | 23.8 | 0.20 | 83.9 | 15.4 | 0.7 | 1.28 |
| | Eq. Calc | 1.00 | 0.12 | 98.2 | 0.10 | 1.68 | 87.9 | 7.43 | 4.69 | 2.73 |
| 550 | Exp | 0.76 | 0.08 | 97.1 | 2.60 | 0.25 | 83.8 | 15.5 | 0.7 | 2.02 |
| | Eq. Calc | 1.00 | 0.12 | 99.6 | 0.06 | 0.33 | 88.0 | 11.1 | 0.95 | 2.85 |
| 600 | Exp | 0.97 | 0.10 | 98.0 | 1.92 | 0.05 | 80.7 | 19.2 | 0.1 | 2.57 |
| | Eq. Calc | 1.00 | 0.12 | 100 | 0.04 | 0.07 | 85.3 | 14.5 | 0.19 | 2.85 |
| 650 | Exp | 1.00 | 0.09 | 99.6 | 0.47 | 0 | 75.0 | 25.0 | 0.0 | 2.62 |
| | Eq. Calc | 1.00 | 0.12 | 100 | 0.03 | 0.01 | 81.9 | 18.0 | 0.04 | 2.82 |
| 700 | Exp | 1.00 | 0.08 | 99.9 | 0.19 | 0 | 70.0 | 30.0 | 0.0 | 2.63 |
| | Eq. Calc | 1.00 | 0.11 | 100 | 0.02 | <0.01 | 78.5 | 21.5 | 0.01 | 2.78 |

**Table 4** Mean experimental process outputs for aqueous urea reactant at S:C = 7 using a bed of $Al_2O_3$ pellets (no Ni-catalyst).

| Temp °C | ppm mass $[NH_4^+]_{cond}$ | Conversions | | Sel. H-products % | | | Sel. C-products % | | | $H_2$ Yield (mol/mol) |
|---|---|---|---|---|---|---|---|---|---|---|
| | | $x_{urea}$ | $x_{H2O}$ | $H_2$ | $NH_3$ | $CH_4$ | $CO_2$ | CO | $CH_4$ | |
| 500 | 93951 | 0.25 | 0.08 | 7.0 | 89.8 | 3.2 | 89.1 | 1.9 | 9.7 | 0.051 |
| 550 | 104222 | 0.33 | 0.07 | 7.7 | 89.4 | 2.9 | 91.4 | 1.6 | 7 | 0.063 |
| 600 | 96632 | 0.29 | 0.07 | 2.4 | 94.5 | 3.0 | 90.7 | 1.5 | 7.8 | 0.018 |
| 650 | 86701 | 0.28 | 0.06 | 6.1 | 91.4 | 2.5 | 90.9 | 1.7 | 7.5 | 0.042 |
| 700 | 94291 | 0.30 | 0.06 | 3.6 | 93.9 | 2.6 | 91.9 | 1.6 | 6.6 | 0.027 |

**Table 5** Mean process outputs during the $NH_3$-water solution catalytic cracking experiments in the temperature range (500-700 °C) using the Ni catalyst. Last column is for comparison of the rates with the equivalent aqueous urea experiment on the basis of same (2H) in the non-water feed. Results at 600 °C obtained with just $Al_2O_3$ pellets are also listed.

| Temp °C | Exp/ Eq. Calc | Mol fract $y_{H2}$ | Conv. $x_{NH3 \rightarrow H2}$ | $H_2$ yield mol/mol $NH_3$ | $NH_3 \rightarrow H_2$ mol s$^{-1}$ | Aq.Urea$\rightarrow H_2$ mol s$^{-1}$ |
|---|---|---|---|---|---|---|
| 500 | Ni Exp. | 0.034 | 0.49 | 0.73 | $7.442 \times 10^{-6}$ | $2.128 \times 10^{-5}$ |
| | Eq. Calc. | 0.067 | 1.00 | 1.5 | N/A | N/A |
| 600 | Ni. Exp. | 0.048 | 0.70 | 1.05 | $1.071 \times 10^{-5}$ | $4.254 \times 10^{-5}$ |
| | $Al_2O_3$ Exp | 0.004 | 0.06 | 0.08 | $8.523 \times 10^{-7}$ | $3.032 \times 10^{-7}$ |
| | Eq. Calc. | 0.067 | 1.00 | 1.5 | N/A | N/A |
| 700 | Ni Exp. | 0.041 | 0.59 | 0.89 | $9.053 \times 10^{-6}$ | $4.36 \times 10^{-5}$ |
| | Eq. Calc. | 0.067 | 1.00 | 1.5 | N/A | N/A |

**Table 6** BET surface area (2 measurement per sample) for the Ni catalyst samples and phase composition from powder XRD spectra analysed with Rietveld refinement (2 spectra per sample).

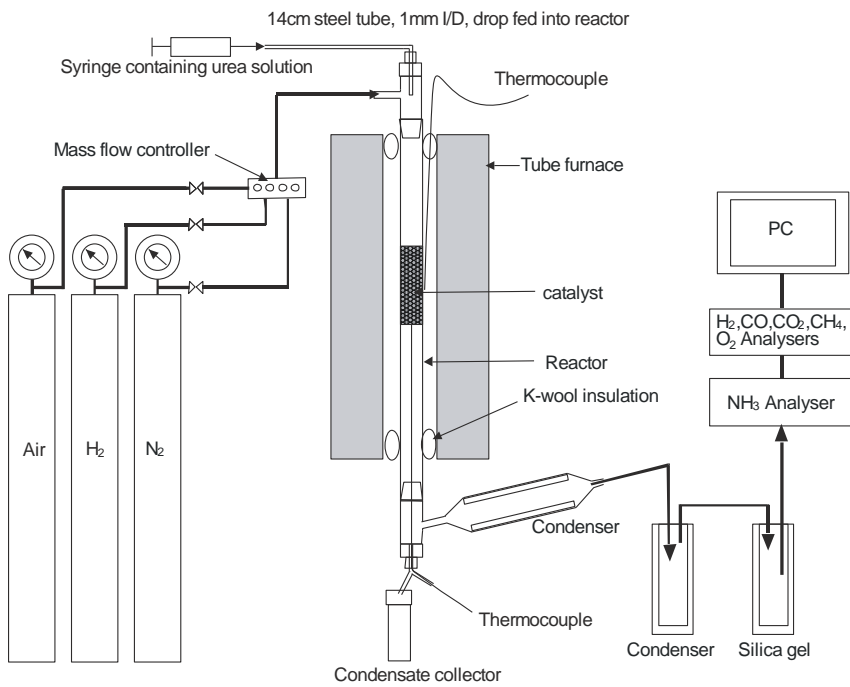| Sample | BET (m$^2$/g) | $Al_2O_3$ (wt%) | NiO (wt%) | Ni (wt%) |
|---|---|---|---|---|
| As-received 1 | 3.262 | 82.0 | 18.0 | 0 |
| As-received 2 | 2.557 | 82.3 | 17.7 | 0 |
| $H_2$-Reduced 1 | 3.720 | 84.1 | 1.6 | 14.3 |
| $H_2$-Reduced 2 | 2.798 | 87.5 | 0 | 12.5 |
| After aq. urea with Ni expts. 1 | 2.775 | 86.4 | 2.7 | 10.9 |
| After aq. urea with Ni expts. 2 | 2.266 | 86.3 | 3.0 | 10.7 |

Figure 1 Diagram of the experimental set up for steam reforming of urea.
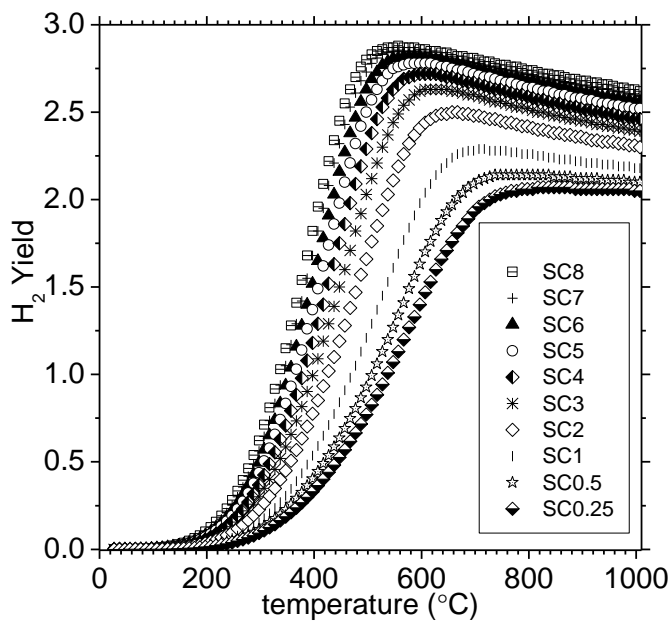


Figure 2  Calculated equilibrium hydrogen yield (mol $H_2$ produced / mol urea in the feed)

as a function of temperature for steam to carbon ratios from 0.25 to 8 and with a fixed $N_2$
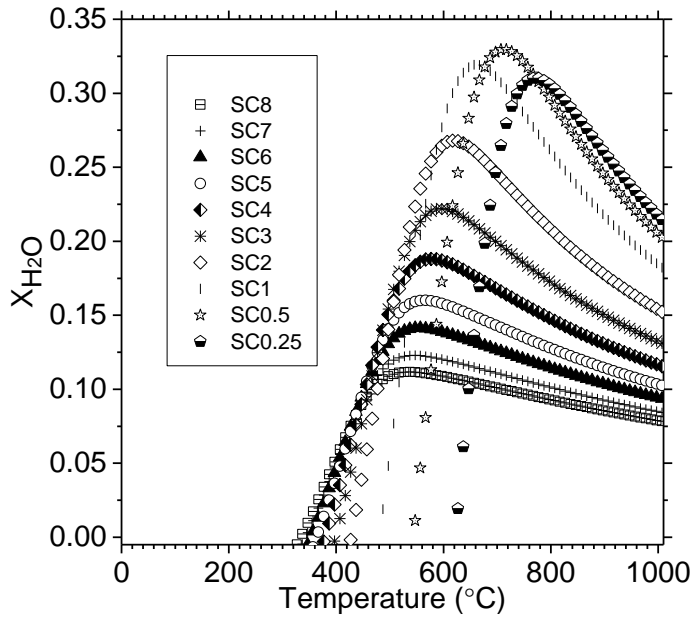
mol fraction of 0.631.

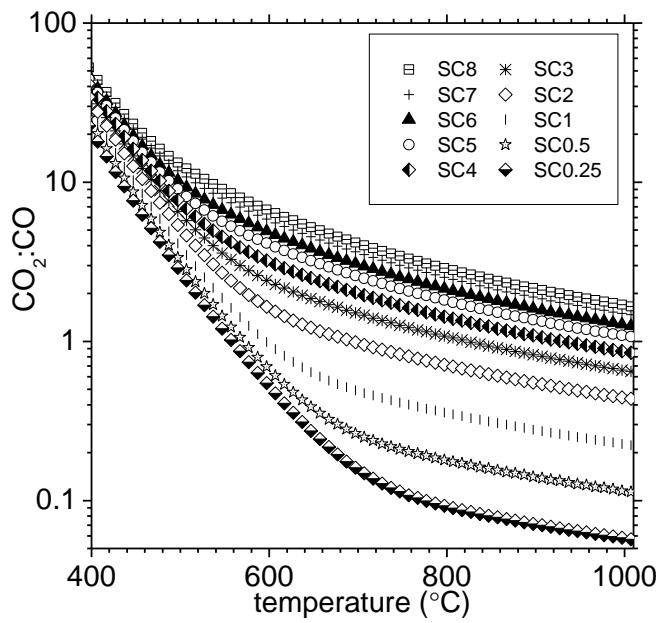Figure 3 Calculated equilibrium steam conversion fraction in same conditions as Fig. 2.



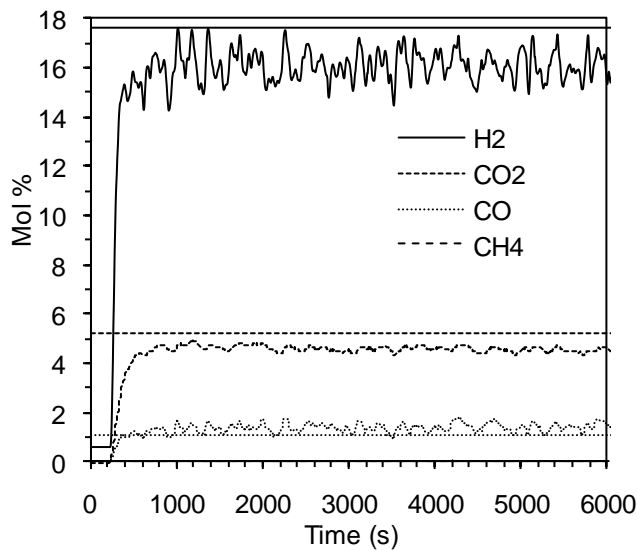Figure 4 Calculated equilibrium $CO_2$ to CO ratio for same conditions as Figs 2 and 3.

Figure 5 Dry gas mol% profiles of $H_2$, CO, $CO_2$ and $CH_4$, 20 g of catalyst, for S:C=6 at 600 °C and calculated equilibrium values. $N_2$ can be calculated by balance to 100%. Straight lines represent the calculated equilibrium values.
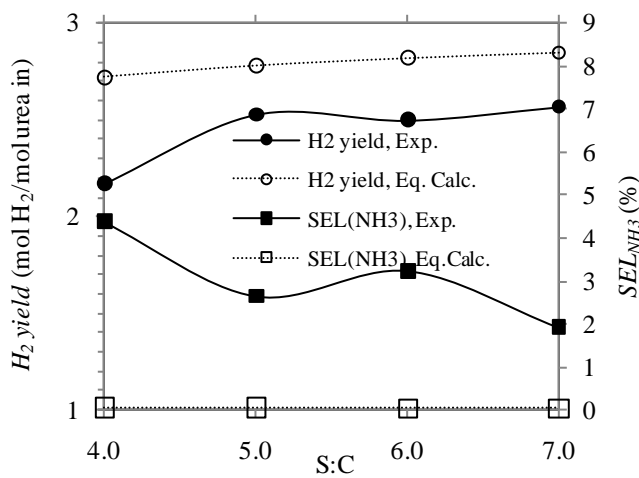


Figure 6 Mean experimental and calculated equilibrium hydrogen yield (mol $H_2$ produced / mol urea in the feed) and $NH_3$ selectivity (%) from H-containing products for steam to carbon ratios from 4 to 7 at 600°C.
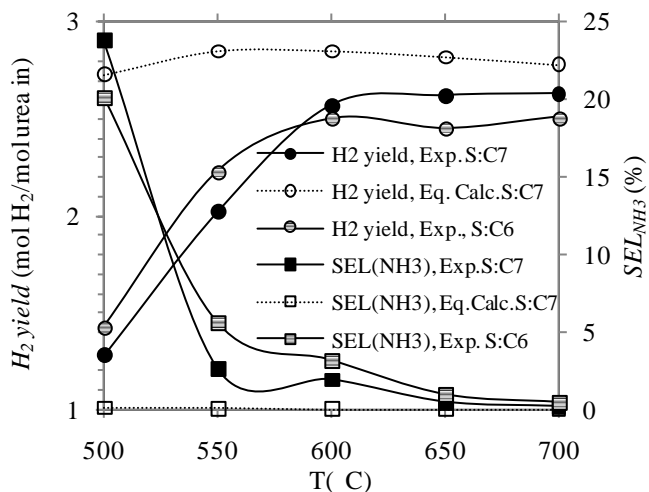
Figure 7 Mean experimental hydrogen yield (mol $H_2$ produced / mol urea in the feed) and NH$_3$ selectivity (%) from H-containing products for temperatures between 500 and 700 °C for steam to carbon ratios of 6 and 7 (solid lines), also includes equilibrium calculated $H_2$ yield and NH$_3$ selectivity for S:C of 7 (dotted lines).
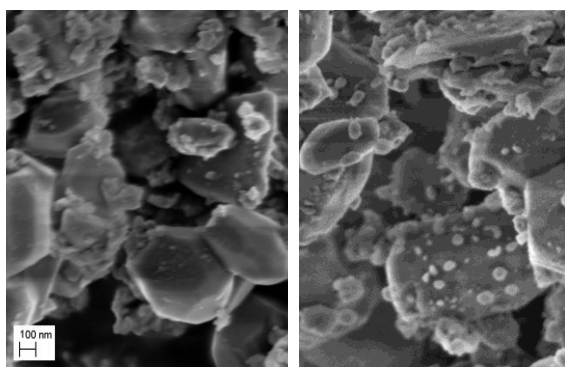


Fig. 8  SEM images of the fresh catalyst after reduction with $H_2$ (left), and after the urea-water experiments, ending with the condition S:C=5 and 500 °C (right).
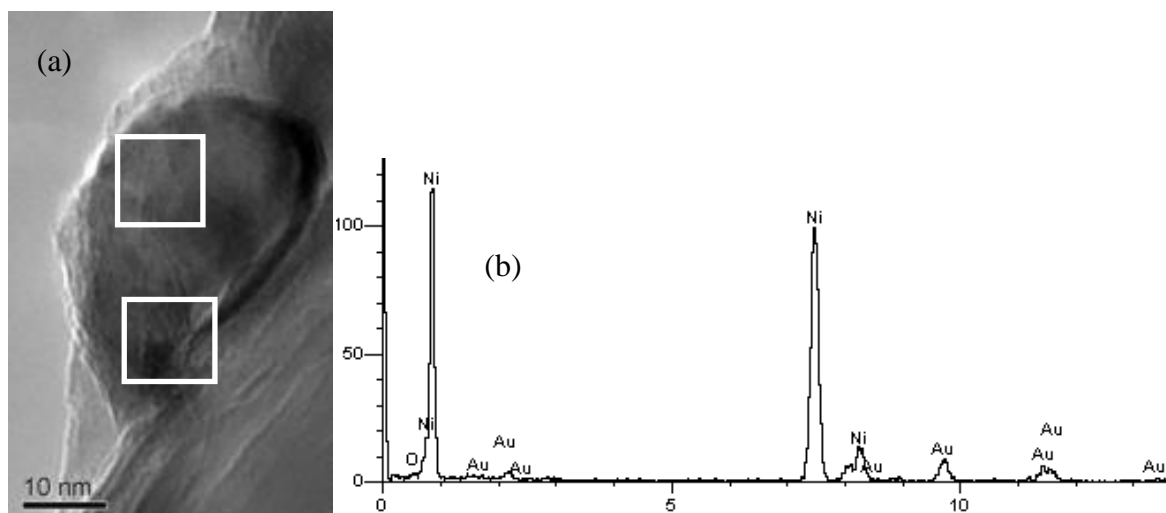
Fig 9  (a) FEGTEM image of surface of catalyst after urea-water experiments, showing square inserts where EDX analysis was carried out and FFT d-spacings were measured, (b) the EDX spectrum indicating the overwhelming presence of Ni. Gold was used as the sample support.
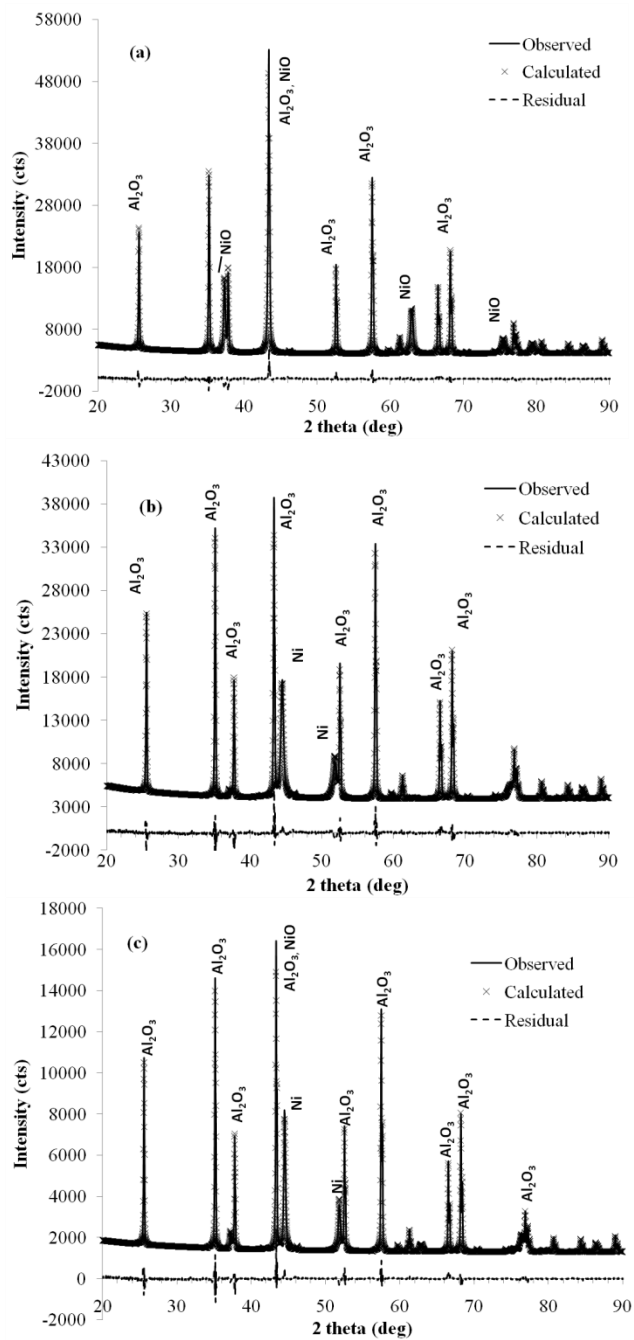
Fig. 10 Powder XRD spectra of the catalyst (a) as-received, (b) following reduction in $H_2/N_2$ flow, (c) after the urea-water experiments. The figures show the measured spectra ('observed') and the modelled spectra calculated by Rietveld refinement ('calculated'). The residual curve (experimental-model) is also shown.